

## Scale invariance of human electroencephalogram signals in sleep

Shi-Min Cai,<sup>1</sup> Zhao-Hui Jiang,<sup>1</sup> Tao Zhou,<sup>2,3,\*</sup> Pei-Ling Zhou,<sup>1</sup> Hui-Jie Yang,<sup>4</sup> and Bing-Hong Wang<sup>2,4</sup>

<sup>1</sup>*Department of Electronic Science and Technology, University of Science and Technology of China, Hefei, Anhui 230026, People's Republic of China*

<sup>2</sup>*Department of Modern Physics, University of Science and Technology of China, Hefei, Anhui 230026, People's Republic of China*

<sup>3</sup>*Department of Physics, University of Fribourg, Chemin du Muse 3, CH-1700 Fribourg, Switzerland*

<sup>4</sup>*Institute of Complex Adaptive Systems, Shanghai Academy of System Science, Shanghai 200093, People's Republic of China*

(Received 12 March 2007; revised manuscript received 25 October 2007; published 5 December 2007)

In this paper, we investigate the dynamical properties of electroencephalogram (EEG) signals of humans in sleep. By using a modified random walk method, we demonstrate that scale-invariance is embedded in EEG signals after a detrending procedure is applied. Furthermore, we study the dynamical evolution of the probability density function (PDF) of the detrended EEG signals by nonextensive statistical modeling. It displays a scale-independent property, which is markedly different from the usual scale-dependent PDF evolution and cannot be described by the Fokker-Planck equation.

DOI: [10.1103/PhysRevE.76.061903](https://doi.org/10.1103/PhysRevE.76.061903)

PACS number(s): 87.19.Nn, 05.40.-a, 89.75.Da

### I. INTRODUCTION

The analysis of electroencephalogram (EEG) signals attracts extensive attention from various research fields, since it cannot only help us to understand the dynamical mechanism of human brain activities, but also be potentially useful in clinics in diagnosing some neural diseases. Some previous work has been done on human EEG signals in sleep and other physiological states. In Refs. [1–3] the correlation dimension and Lyapunov exponent were calculated to characterize and discriminate the sleep stages. Lee *et al.* provided evidence for the long-range power-law correlations embedded in EEG signals [4]. The mean scaling exponents were distinguished according to rapid eye movement (REM), non-REM, and awake stages, and gradually increased from stage 1 to stages 2, 3, and 4 in non-REM sleep. Hwa *et al.* found a variable scaling behavior in two regions, and described the topology plot of the scaling exponents in these two regions, which reveals the spatial structure of the nonlinear electronic activity [5]. Random matrix theory is used to demonstrate the existence of generic and subject-independent features of the ensemble of correlation matrices extracted from human EEG signals [6]. Yuan *et al.* found similar long-range temporal correlations and power-law distribution of the increments of EEG signals after filtering out the  $\alpha$  and  $\beta$  waves [7].

Furthermore, some very recent work [8,9] pointed out that the sleep-wake transitions exhibit a scale-invariant pattern and embed a self-organized criticality (see also Ref. [10] for the concept of self-organized criticality). In the present paper, the Tsallis entropy is used to analyze a series of human EEG signals in sleep. Robust scale invariance was discovered for the EEG signals of brains in sleep, which does, to some extent, indicate that the human brain activity in sleep may be related to a self-organized critical system.

We use the Massachusetts Institute of Technology (MIT)–Beth Israel Hospital (BIH) polysomnographic database,

which is a collection of recordings of multiple physiological signals during sleep. Subjects were monitored in Boston's Beth Israel Hospital Sleep Laboratory for evaluation of chronic obstructive sleep apnea syndrome, and to test the effects of constant positive airway pressure, a standard therapeutic intervention that usually prevents or substantially reduces airway obstruction in these subjects. The database contains four-, six-, and seven-channel polysomnographic recordings, each with an electrocardiogram (ECG) signal annotated beat by beat, and with an EEG signal annotated with respect to sleep stages [12]. The records were digitized at a sampled interval of 250 Hz and 12 bits precision. The polysomnographic wave forms were displayed on CRT display and edited by using a program called WAVE (wave-form analysis, viewer, and editor), which was developed at Massachusetts Institute of Technology. The sleep stage was annotated at 30 s intervals according to the criteria of Rechtschaffen and Kales, denoted by six discrete levels—1, 2, 3, 4, REM, and awake (stages 1, 2, 3, and 4 belong to non-REM sleep) [13]. More details of the MIT-BIH polysomnographic database collection can be found in Ref. [14]. In this paper, we chose the experimental data with the criterion that the subject record contain at least five states, with the persistent length of the state larger than  $10^5$ . Under this criterion, we chose ten subjects, and in total 40 samples: nine samples for the awake state, eight samples for the REM state, five samples for stage 1, nine samples for stage 2, six samples for stage 3, and three samples for stage 4. The testers in the experimental procedure were patients with diseases like obstructive apnea with arousal, hypopnoea with arousal, and obstructive apnea. However, the disease status could only be observed in a short time period during the transition between states. The chosen experimental data were required to cover sufficiently long time periods in which the testers did not detect the disease. The average length of records in each stage was larger than  $10^5$ . The smallest average length was  $1.21 \times 10^5$  for stage 3 (corresponding to 7 min), while the largest contained  $4.525 \times 10^5$  samples for the awake stage (corresponding to 28 min). A representative example is shown in Fig. 1. In addition to Fig. 1, all the experimental

\*zhutou@ustc.edu

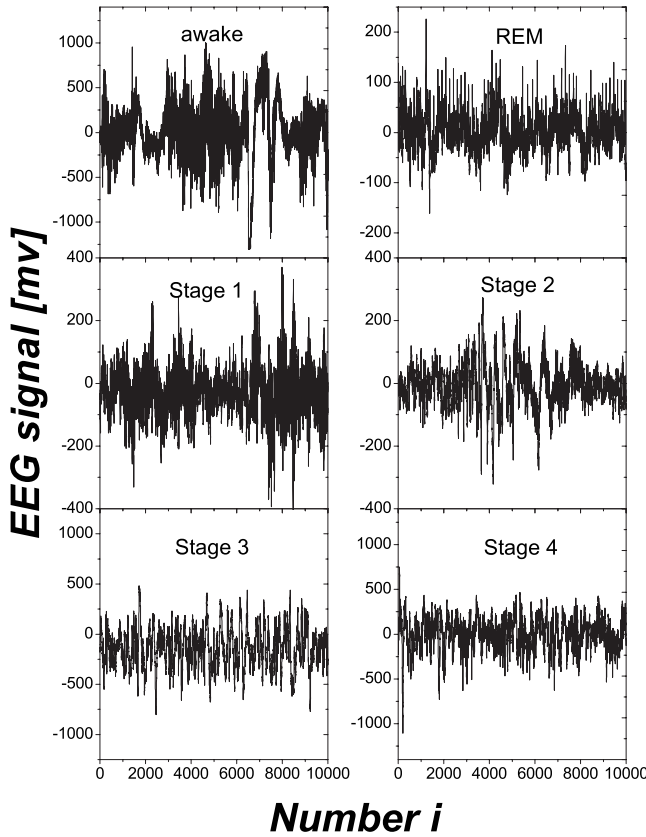


FIG. 1. A set of representative records of EEG signals in different stages. Each entire experimental data set includes more than  $10^5$  data points, while only a small fraction are plotted.

results shown in this paper were obtained by averaging over the ten chosen subjects.

## II. SCALE INVARIANCE OF DETRENDED EEG SIGNALS

Consider an EEG series, denoted by  $\{x_i\}$  ( $i=1, 2, \dots, N$ ), whose scaling characteristics are detected through the following procedure.

*Step 1.* We construct the profile series  $Y_j = \sum_{i=1}^j x_i$ ,  $j = 1, 2, \dots, N$ , and consider  $Y_j$  as the *walk displacement* of the resulting random walk.

*Step 2.* We divide the profile series into nonoverlapping segments with equal length and fit each segment with a second-order polynomial function. We regard the fitting results as trends; a stationary series can be obtained by eliminating the trends from the profile series.

*Step 3.* After the detrending procedure, we define the increment of this modified profile series at a scale  $s$  as  $\Delta_s Y_j = Y_{j+s}^* - Y_j^*$ , where  $Y_j^*$  is the deviation from the polynomial fit.

*Step 4.* Scale invariance (self-similarity) in the stationary series implies that the probability distribution function (PDF) satisfies

$$P(x, s) = \frac{1}{\sigma_s} P\left(\frac{x}{\sigma_s}\right), \quad (1)$$

where  $\sigma_s$  denotes the standard deviation at time scale  $s$ . Obviously,  $P(0, s) = P(0)1/\sigma_s$ .

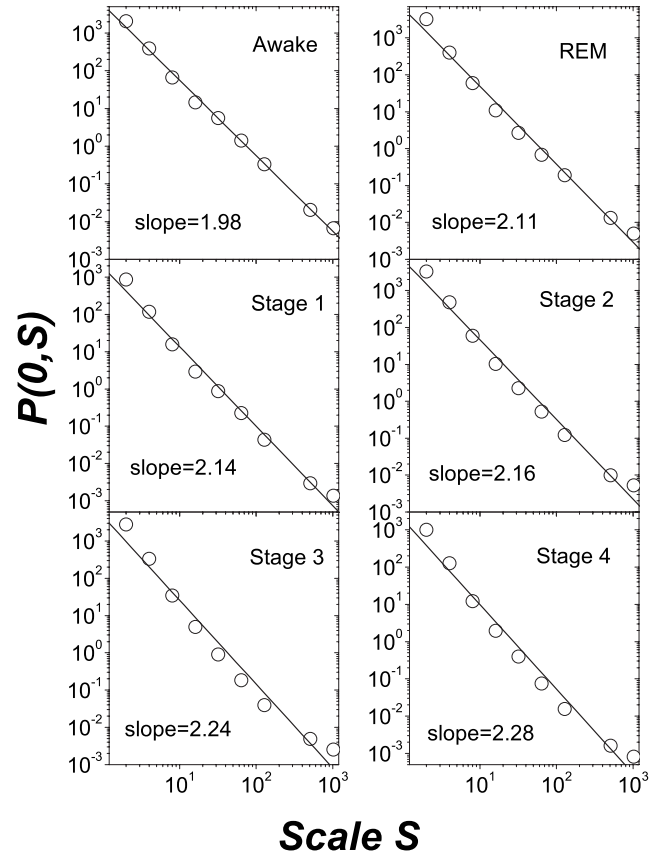


FIG. 2.  $P(0, s)$  as a function of the time sampling scale  $s$ . A power-law scaling behavior is observed for about three orders of magnitude. The data points for awake, REM, and stages 1, 2, 3, and 4 are obtained by averaging nine, eight, five, nine, six, and three samples, respectively.

Changing the time scale  $s$  from  $2^1$  to  $2^{10}$ , the normalized PDFs of  $\Delta_s Y$  exhibit scale-invariant (self-similar) behaviors as presented in Fig. 2. That is to say, those PDFs can be rescaled into a single master curve, as shown in Fig. 3. The scale invariance of the detrended EEG signals suggests that a quasistationary property is embedded in the distributions of time scales. Therefore, it helps us to search for stable distributions to mimic them.

## III. NONEXTENSIVE STATISTICAL MODELING OF DETRENDED EEG SIGNALS

From the results sketched in the preceding section, here we use the Tsallis entropy to model the PDFs. The Tsallis entropy was introduced by Tsallis through generalizing the standard Boltzmann-Gibbs theory [15], and is given by

$$S_q = k \frac{1 - \int dx [p(x)]^q}{q - 1} \quad \left( \int dx p(x) = 1, q \in R \right). \quad (2)$$

In the limit  $q \rightarrow 1$ ,  $S_q$  degenerates to the Boltzmann-Gibbs-Shannon entropy as

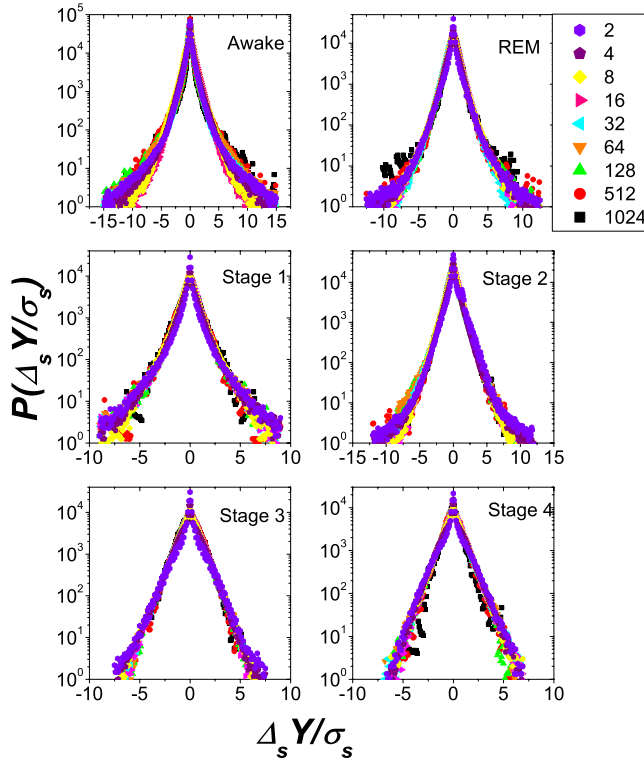


FIG. 3. (Color online) Rescaled increment PDFs for six stages. Obviously, curves with different time scales can well collapse onto a single master curve, demonstrating the existence of a quasistationary property. The different values of the time scale  $s$  are presented in the right panel, increasing as 2, 4, 8, ..., 1024. The data points for awake, REM, and stages 1, 2, 3, and 4 are obtained by averaging nine, eight, five, nine, six, and three samples, respectively.

$$S_1 = - \int p(x) \ln[p(x)] dx. \quad (3)$$

The optimization of  $S_q$  (i.e., maximal  $S_q$  if  $q > 0$ , and minimal  $S_q$  if  $q < 0$ ) with the normalization condition  $\int dx p(x) = 1$ , as well as the constraint  $\langle \langle x^2 \rangle \rangle_q = \sigma^2$ , leads to the  $q$ -Gaussian distribution ( $q < 3$ )

$$G_q(x, s) = \frac{1}{Z_q(s)} (1 - \beta(s) \{ (1 - q) [x - \bar{x}(s)]^2 \}_+^{1/1-q}), \quad (4)$$

where  $Z_q(s)$  is a normalization constant,  $\beta(s)$  is explicitly related to the variance of the distribution, and the subscript + indicates that  $G_q(x, s)$  is non-negative [16].  $G_{q \rightarrow 1}(x, s)$  recovers the usual Gaussian distribution. The  $q$ -Gaussian PDF can describe a set of stable distributions from Gaussian to Lévy regimes [17] by adjusting the value of  $q$  with appropriate time-dependent parameters  $\beta(s)$  and  $Z_q(s)$  [18]. The distribution falls into the Lévy regime in the interval  $5/3 < q < 3$ , with  $q = 5/3$  the critical value.

The results in Fig. 4 show that the PDF of the awake stage falls into the Lévy regime with  $q$  being equal to 1.94. It exhibits sharp kurtosis and a long-tail distribution, distinguished from those of REM and non-REM stages. It should

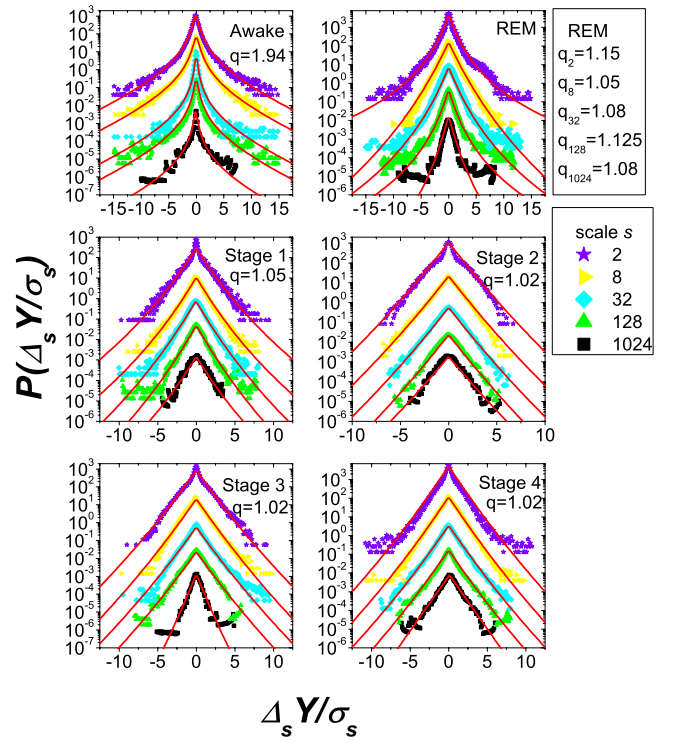


FIG. 4. (Color online) Rescaled increment PDFs of all stages with the approximate fit using nonextensive statistical modeling. We use a  $q$ -Gaussian function to fit the awake stage, and a  $q$ -exponential function to fit other five stages. The awake stage falls into the Lévy regime with the best-fit parameter  $q = 1.94$ . In the REM stage, the values of  $q$  are slightly different; while in each non-REM stage, they are almost the same. All the data points for awake, REM, and stages 1, 2, 3, and 4 are obtained by averaging nine, eight, five, nine, six, and three samples, respectively.

be noted that we shift the distributions by dividing them by their standard deviations and plot only the cases of time scale  $s = 2, 8, 32, 128, 1024$  to make the figure clear.

The specific values of  $\beta(s)$  for all scales are shown in Fig. 5. Interestingly,  $\beta(s)$  does not dissipate as the time scale  $s$  increases, unlike the behavior of  $\beta(s)$  recently reported in financial markets (see Fig. 11 in Ref. [19]), in which  $\beta(s)$  decreases in a power-law form with time scale  $s$ , indicating scale-dependent PDF evolution. In other words, it demonstrates that the dynamical evolution of EEG signals is not coincident with the diffusion process described by the Fokker-Planck equation [20].

Another significant equation of the nonextensive statistical approach is the  $q$ -exponential function, which reads

$$e_q(x, s) = \frac{1}{Z_q(s)} \{ 1 - \tau(s) [(1 - q) |x - \bar{x}(s)|] \}_+^{1/1-q}, \quad (5)$$

where the parameter  $\tau(s)$  is the relaxation rate of the distribution. Clearly, in the limit  $q \rightarrow 1$ ,

$$e_1(x, s) = \frac{1}{Z_q(s)} \exp[-\tau(s) |x - \bar{x}(s)|]. \quad (6)$$

Because the statistical distributions of the detrended increments of EEG signals in the sleep stages exhibit an approxi-

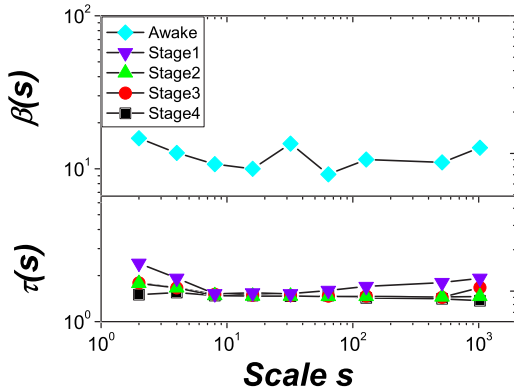


FIG. 5. (Color online)  $\beta(s)$  and  $\tau(s)$  versus  $s$  for awake and non-REM stages. The values of  $\beta(s)$  do not dissipate as  $s$  increases. In particular,  $\tau(s)$  of non-REM sleep converges to an invariant pattern. All the data points for awake and stages 1, 2, 3, and 4 are obtained by averaging nine, five, nine, six, and three samples, respectively.

mately exponential form, we use the  $q$ -exponential model to quantify them, as shown in Fig. 4. The values of  $q$  for the REM and the non-REM stages are a little bit larger than 1. This means that the fluctuation of human brain activities in the sleep stage converges to a normal exponential pattern. In particular, the EEG signals exhibit a  $q$ -invariant pattern for different time scales in all the four stages within non-REM sleep. The relaxation rates of the distributions are also approximately invariant, as shown in Fig. 5. However, in the REM stage, the values of  $q$  change slightly, and only the center part of the distribution can be well fitted by the present model. This irregularity of brain electrical activity in the REM stage may result from the acute neural activity [21].

The nonextensive statistical approach, modeling the detrended increment's PDF of EEG signals with an invariant parameter  $q$ , demonstrates the scale-independent property of the system. In order to further test the existence of this observed property, we randomize the empirical series of the awake stage by shuffling [22,23] and show a fit for this artificial distributions at different scales in Fig. 6. Clearly, the parameter  $q$  will approach the Gaussian regime ( $q=1$ ) as the time scale increases. This result strongly illuminates that the scale-independent property of human brain activity in sleep is remarkably different from the turbulentlike scale-dependent evolution [24]. Since the fluctuation in a system near a critical point is generally associated with scale invariance, the existence of a scale-dependent property of EEG signals indicates that the human brain activity in sleep may be related to a self-organized critical system, supporting a prior report about this issue [11].

#### IV. CONCLUSION

In this paper, several dynamical properties of human EEG signals in sleep are investigated. We first use a modified random walk method to construct the profile series including the information of the EEG signals. After a detrending procedure, we obtain a stationary series and define the increments

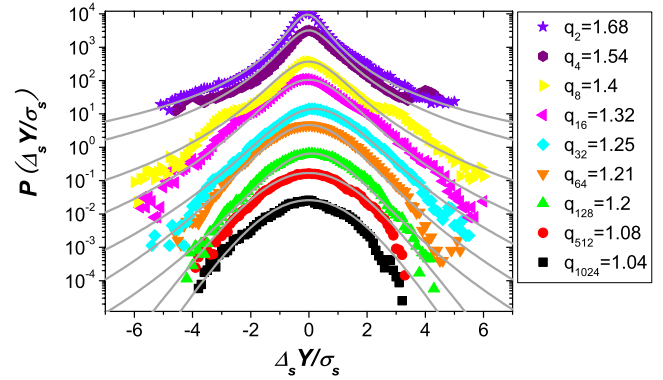


FIG. 6. (Color online) Increment PDF of randomized series of awake stage and fitting curves with different parameters  $q$ . The parameter  $q$  rapidly approaches the Gaussian regime ( $q=1$ ) as the time scale increases. For clarity, we shifted the distributions by dividing them by their standard deviations.

of the resulting random walk at multiple scales. In order to characterize the dynamical process of brain electronic activity, we then study the  $P(0, s)$  of the PDF of normalized increments as a function of  $s$ . With this choice we investigate the point of each probability distribution that is least affected by the noise introduced by the experimental data set. Scale invariance in both awake and sleep stages is obtained; thus one can rescale the distributions at different scales into a single master curve.

Aiming to investigate this property, we use the nonextensive statistical approach to model these processes. The dynamical evolution of the detrended increments' PDF in the awake stage can be well fitted by the  $q$ -Gaussian distribution with an invariant parameter  $q=1.94$ . It demonstrates that the PDFs of the awake stage fall into the Lévy regime. In contrast, a  $q$ -exponential distribution is used to mimic the PDFs of the sleep stages. In particular, the non-REM stage exhibits scale-independent distributions; while for the REM stage, the analysis suggests a complex distributional form with slightly different values of  $q$ . Note that, in many prior quantitative methods, like entropy and Lyapunov estimates, the REM and awake states are indistinguishable based on the entire time scale. Instead, here we analyze the EEG series at different time scales, and find a great difference of the  $q$  value in the awake state (i.e.,  $q=1.94$ ), which may be due to the extreme neural activity. However, the real biological reason is not clear thus far. We hope this sharply different  $q$  value can reveal some information that could be useful for a future and in-depth exploration.

In a recent work [24], Lin and Hughson proposed a turbulentlike cascade model, which describes a scale-dependent PDF evolution, to mimic the human heart rate; the validity of the model is, now, being challenged by the critical scaling invariance found in real human heart-rate processes [25,26]. In this paper, we demonstrate that the process of brain electric activity is remarkably different from a turbulentlike cascade evolution, similar to what was found by Kiyonol *et al.* [25,26]. It is generally accepted that the complex dynamics of the heart rate is caused by an intricate balance between the two branches of the autonomic nervous system: the parasymp-



pathetic (PNS) and the sympathetic (SNS) nervous systems, which respectively decrease and increase the heart rate. The autonomic nervous system is controlled by the central nervous system of the brain. Therefore, even though the electrocardiograph and electroencephalogram are different, their similarities may not be a coincidence. Although the comparison of the EEG and ECG in this paper could not present a convincing link between the scale-invariant properties of heart rate and EEG, the discussion of this aspect may enlighten readers and can provide some insights into the underlying dynamical mechanism of brain activity. In addition,

like the corresponding empirical studies on human ECG signals, this work could provide some criteria for theoretical models of human EEG signals.

#### ACKNOWLEDGMENTS

This work is supported by the National Natural Science Foundation of China under Grants No. 70571075, No. 70571074, and No. 10635040. B.H.W. acknowledges 973 Project 2006CB705500.

- 
- [1] J. Fell and J. Röschke, *Int. J. Neurosci.* **76**, 109 (1994).  
 [2] J. Fell, J. Röschke, K. Mann, and C. Schaffner, *Clin. Neurophysiol.* **98**, 401 (1996).  
 [3] T. Kobayashi, S. Madokoro, T. Ota, H. Ihara, Y. Umezawa, J. Murayama, H. Kosada, K. Misaki, and H. Nakagawa, *Psychiatry Clin. Neurosci.* **54**, 278 (2000).  
 [4] J. M. Lee, D. J. Kim, I. Y. Kim, K. S. Park, and S. I. Kim, *Comput. Biol. Med.* **32**, 37 (2002).  
 [5] R. C. Hwa and T. C. Ferree, *Phys. Rev. E* **66**, 021901 (2002).  
 [6] P. Šeba, *Phys. Rev. Lett.* **91**, 198104 (2003).  
 [7] J. W. Yuan, B. Zheng, C. P. Pan, Y. Z. Wu, and S. Trimper, *Physica A* **364**, 315 (2006).  
 [8] C. C. Lo, T. Chou, T. Penzel, T. E. Scammell, R. E. Strecker, H. E. Staney, and P. C. Ivanov, *Proc. Natl. Acad. Sci. U.S.A.* **101**, 17545 (2004).  
 [9] J. C. Comte, P. Ravassard, and P. A. Salin, *Phys. Rev. E* **73**, 056127 (2006).  
 [10] P. Bak, *How Nature Works: The Science of Self-Organized Criticality* (Springer, New York, 1996).  
 [11] L. de Arcangelis, C. Perrone-Capano, and H. J. Herrmann, *Phys. Rev. Lett.* **96**, 028107 (2006).  
 [12] A. L. Goldberger, L. A. N. Amaral, L. Glass, J. M. Hausdorff, P. C. Ivanov, R. G. Mark, J. E. Mietus, G. B. Moody, C. K. Peng, and H. E. Stanley, *Circulation* **101**, e215 (1999).  
 [13] A. Rechtschaffen and A. Kales, *A Manual of Standardized Terminology, Techniques and Scoring System for Sleep Stage of Human Subjects* (U.S. Dept. of Health, Education, and Welfare, Bethesda, MD, 1968).  
 [14] Y. Ichimaru and G. B. Moody, *Psychiatry Clin. Neurosci.* **53**, 175 (1999).  
 [15] C. Tsallis, *J. Stat. Phys.* **52**, 479 (1988).  
 [16] S. Abe and Y. Okamoto, *Nonextensive Statistical Mechanics and Its Application* (Springer, Berlin, 2001).  
 [17] P. Lévy, *Théorie de l'Addition des Variables Aléatoires* (Gauthier-Villars, Paris, 1927).  
 [18] C. Vignat and A. Plastino, *Phys. Rev. E* **74**, 051124 (2006).  
 [19] A. A. G. Cortines and R. Riera, *Physica A* **377**, 181 (2007).  
 [20] The Fokker-Planck equation is used to describe a scale-dependent evolution process with asymptotic power-law relation  $\beta(s) \sim s^\alpha$ .  
 [21] E. R. Kandel, J. H. Schwartz, and T. M. Jessell, *Principles of Neural Science* (McGraw-Hill, New York, 2000).  
 [22] J. Theiler, S. Eubank, A. Longtin, B. Galdrikian, and J. D. Farmer, *Physica D* **58**, 77 (1992).  
 [23] J. Theiler and D. Prichard, *Physica D* **94**, 221 (1996).  
 [24] D. C. Lin and R. L. Hughson, *Phys. Rev. Lett.* **86**, 1650 (2001).  
 [25] K. Kiyono, Z. R. Struzik, N. Aoyagi, S. Sakata, J. Hayano, and Y. Yamamoto, *Phys. Rev. Lett.* **93**, 178103 (2004).  
 [26] K. Kiyono, Z. R. Struzik, N. Aoyagi, F. Togo, and Y. Yamamoto, *Phys. Rev. Lett.* **95**, 058101 (2005).